Determining the role of novel metabolic pathways in driving intracranial pressure reduction after weight loss

Alimajstorovic, Zerin; Mitchell, James; Yiangou, Andreas; Hancox, Thomas; Southam, Andrew; Grech, Olivia; Ottridge, Ryan; Winder, Cate; Tahrani, Abd; Tan, Tricia M.; Mollan, Susan; Dunn, Warwick; Sinclair, Alex

DOI:
10.1093/braincomms/fcad272

Determining the role of novel metabolic pathways in driving intracranial pressure reduction after weight loss.

Zerin Alimajstorovic[1], James L. Mitchell[1,2], Andreas Yiangou[1,2], Thomas Hancox[3], Andrew D. Southam[3], Olivia Grech[1], Ryan Ottridge[4], Catherine L. Winder[3,5], Abd A. Tahrani[1,6], Tricia M. Tan[7], Susan P. Mollan[1,8], Warwick B. Dunn[1,3,5] and Alexandra J Sinclair[1,6,8]

Author affiliations:

1 Institute of Metabolism and Systems Research, College of Medical and Dental Sciences, University of Birmingham, Birmingham, UK

2 Department of Neurology, University Hospitals Birmingham NHS Foundation Trust, Queen Elizabeth Hospital, Birmingham, UK.

3 School of Biosciences, College of Life and Environmental Sciences, University of Birmingham, Birmingham, UK.

4 Birmingham Clinical Trials Unit, College of Medical and Dental Sciences, University of Birmingham, Birmingham, UK.

5 Department of Biochemistry and Systems Biology, Institute of Systems, Molecular, and Integrative Biology, University of Liverpool, UK

6 Centre for Endocrinology, Diabetes and Metabolism, Birmingham Health Partners, Birmingham, UK.

7 Section of Endocrinology and Investigative Medicine, Department of Metabolism, Digestion and Reproduction, Faculty of Medicine, Imperial College London, London, UK.

8 Birmingham Neuro-Ophthalmology, University Hospitals Birmingham, Queen Elizabeth Hospital, Birmingham, UK.

Correspondence to: Professor Alexandra Sinclair

Institute of Metabolism and Systems Research, College of Medical and Dental Sciences, University of Birmingham, Birmingham, B15 2TT, United Kingdom.

a.b.sinclair@bham.ac.uk

Running title: IIH metabolic pathways involved in ICP.

Abstract

Idiopathic intracranial hypertension, a disease classically occurring in women with obesity, is characterised by raised intracranial pressure. Weight loss leads to reduction in intracranial pressure. Additionally, pharmacological glucagon-like peptide-1 agonism reduces cerebrospinal fluid secretion and intracranial pressure. The potential mechanisms by which weight loss reduces intracranial pressure are unknown and was the focus for this study.

Meal stimulation tests (fasted plasma sample, then samples at 15, 30, 60, 90 and 120 minutes following a standardised meal) were conducted pre- and post-bariatric surgery (early (2 weeks) and late (12 months)) in patients with active idiopathic intracranial hypertension. Dynamic changes in gut neuropeptides (glucagon-like peptide-1, gastric inhibitory polypeptide, and ghrelin) and metabolites (untargeted ultra-high performance liquid chromatography-mass spectrometry) were

evaluated. We determined the relationship between gut neuropeptides, metabolites, and intracranial pressure.

18 idiopathic intracranial hypertension patients were included (Roux-En-Y gastric bypass n=7, gastric banding n=6, or sleeve gastrectomy n=5). At 2 weeks post-bariatric surgery, despite similar weight loss, Roux-En-Y gastric bypass had a two-fold (50%) greater reduction in intracranial pressure compared to sleeve. Increased meal stimulated glucagon-like peptide-1 secretion was observed after Roux-En-Y gastric bypass (+600 %) compared to sleeve (+319 %). There was no change in gastric inhibitory polypeptide and ghrelin. Dynamic changes in meal stimulated metabolites after bariatric surgery consistently identified changes in lipid metabolites, predominantly ceramides, glycerophospholipids and lysoglycerophospholipids, which correlated with intracranial pressure. A greater number of differential lipid metabolites were observed in the Roux-En-Y gastric bypass cohort at 2 weeks, and these also correlated with intracranial pressure.

In idiopathic intracranial hypertension, we identified novel changes in lipid metabolites and meal stimulated glucagon-like peptide-1 levels following bariatric surgery which were associated with changes in intracranial pressure. Roux-En-Y gastric bypass was most effective at reducing intracranial pressure despite analogous weight loss to gastric sleeve at 2 weeks post-surgery and was associated with more pronounced changes in these metabolite pathways. We suggest that these novel perturbations in lipid metabolism and glucagon-like peptide-1 secretion are mechanistically important in driving reduction in intracranial pressure following weight loss in patients with idiopathic intracranial hypertension. Therapeutic targeting of these pathways, for example with glucagon-like peptide-1 agonist infusion, could represent a therapeutic strategy.

Keywords: Pseudotumor cerebri; metabolomics; meal stimulation; bariatric surgery.

Introduction

Idiopathic intracranial hypertension (IIH) is a disease of raised intracranial pressure (ICP).[1, 2] Symptoms of IIH include disabling daily headaches and visual disturbances, with papilloedema leading to permanent visual loss in up to 40% of patients.[1, 3-5] The underlying pathogenesis of IIH is not fully understood but the disease occurs predominantly in women with obesity[6, 7] and the incidence of IIH is increasing in line with country specific obesity rates.[8, 9] IIH disease activity, as measured by ICP, correlates closely with truncal adiposity.[10, 11] Weight loss is therapeutic in IIH and reduces ICP.[12, 13] However, the mechanism by which weight loss reduces ICP is not known. In IIH, there is systemic metabolic dysregulation in excess to that predicted by obesity, including insulin resistance and hyperleptinaemia.[10, 14] In addition, a distinct profile of androgen excess and glucocorticoid dysregulation have been noted.[15-17] These factors may drive the increased risk of cardiovascular disease (CVD), type 2 diabetes mellitus (T2D),[9] obstructive sleep apnoea,[14] reduced fertility, gestational diabetes and pre-eclampsia[18, 19] compared with age, sex, body mass index matched populations, in IIH. Additionally, metabolic dysregulation has been noted in association with the severe headaches observed in IIH.[20-22]

The gut neuropeptide glucagon-like peptide-1 (GLP-1) is of interest in IIH. GLP-1 is an incretin hormone secreted in the gut and is known to stimulate insulin secretion and inhibits glucagon release.[23, 24] GLP-1 is also synthesized in neurons of the nucleus tractus solitarius that project to the hypothalamus[25] and promotes satiety and weight loss.[26] In vivo data has identified GLP-1 receptor (GLP-1R) expression in the human and rodent choroid plexus.[27, 28] The GLP-1 receptor

agonist, Exenatide, directly reduces cerebrospinal fluid secretion and ICP in vivo.[27] Consequently, GLP receptor agonism has been investigated as a potential target for treating conditions with raised ICP such as IIH. A randomised double-blind placebo controlled trial in patients with active IIH demonstrated that Exenatide significantly reduced ICP in IIH at 2.5 hours, 24 hours and at 12 weeks,[29] suggesting a weight-independent and direct effect of GLP-1R agonsim on ICP in IIH.

Bariatric surgery has been shown to significantly reduce ICP in association with the amount of weight loss, in IIH, in a randomised clinical trial (IIH:WT).[12, 30] Weight loss and ICP reduction was most pronounced in those undergoing Roux-En-Y gastric bypass (RYGB).[7] Different types of bariatric surgery are known to have differing effects on GLP-1 secretion with the most pronounced changes occurring in those undergoing RYGB surgery, a procedure which bypasses food to the mid/distal jejunum and exposes L-cells to nutrients which trigger a sharp rise in GLP-1, oxyntomodulin and peptide YY.[31, 32] In contrast, sleeve gastrectomy leads to accelerated gastric emptying which also triggers increased GLP-1 secretion, but less marked peptide YY secretion.[31-34]

In the IIH bariatric surgery trial (IIH:WT) it was observed that the amount of weight loss was significantly correlated with the degree of reduction in ICP.[30] Of interest, however, was the observation that ICP was very rapidly reduced (at two weeks) after bariatric surgery, and this appeared to be predominantly independent of weight loss as only relatively small changes in body weight had occurred at this time point.[12] This observation is akin to the early improvements in glycaemic control noted at two weeks post-bariatric surgery in patients with T2D, which were predominantly noted amongst those undergoing RYGB surgery. In T2D this phenomenon has been linked to the increased post-prandial GLP-1, oxyntomodulin and peptide YY secretion.[31, 32]

In this study, we hypothesized that the therapeutic efficacy of weight loss in IIH may be driven by changes in metabolism and gut neuropeptides such as GLP-1. We sought to gain an understanding of the mechanisms underlying the reduction in ICP in people with IIH following bariatric surgery through evaluation of gut neuropeptide and metabolic profiles, by applying untargeted ultra-high performance liquid chromatography-mass spectrometry (UHPLC-MS) metabolomic analysis, over the course of a meal stimulation test. We then determined if the type of bariatric surgery had a differential effect on metabolism (at 2 weeks (early) and 12 months (late)) following surgery. Finally, we aimed to study the relationship between gut neuropeptides, metabolites and ICP.

Materials and methods

Study type

This was a pre-planned sub-analysis of the IIH:WT randomised control trial.[35] This trial identified and recruited IIH subjects from neurology and ophthalmology clinics from seven United Kingdom National Health Service hospitals. These sites as well as the clinical trial protocol and results have been published elsewhere[12, 35, 36] and received ethical approval from the National Research Ethics Committee West Midlands – The Black Country REC (14/WM/0011, Dudley, United Kingdom). All participants provided written informed consent.

Trial details

IIH:WT was funded by the National Institute for Health and Care Research (NIHR-CS-011-028) and registered with ClinicalTrials.gov: NCT02124486.

Study population

The eligibility criteria for the main IIH:WT have previously been published.[35] In brief, this included women aged 18-55 years, with a body mass index (BMI) ≥35 kg/m^2 and active IIH (lumbar puncture opening pressure >25 cmCSF and Frisén papilloedema grade ≥1).[12, 35] For this sub-study, additional eligibility criteria included being randomised to the bariatric surgery arm of the trial (RYGB, gastric sleeve or gastric band[12, 35]) and consenting to undergo meal stimulation testing.

Clinical assessments

The IIH participants attended for trial visits at baseline, 2 weeks post-surgery and at 12 months, according to the published protocols.[35] All participants underwent detailed medical history and clinical examination including a pregnancy test. BMI was calculated from weight and height using the following formula: BMI = (weight [kg] / height [m]^2). Visual tests performed included the perimetric mean deviation (PMD) using Humphrey 24-2 Swedish Interactive Thresholding Algorithm (SITA)[37] central threshold automated perimetry and spectral domain optical coherence tomography (OCT; Spectralis, Heidelberg Engineering) imaging to evaluate the average peripapillary retinal nerve fibre layer (RNFL), a measure of papilloedema.[38] Monthly headache days and headache severity were recorded using headache diaries and headache associated disability was measured using the headache impact test-6 score (HIT-6). Lumbar punctures were conducted at baseline, 2 weeks post-surgery and at 12 months using a standardised procedure in the lateral decubitus position under ultrasound guidance with lumbar puncture opening pressure recorded.[12, 35]

Meal stimulation

Meal stimulation tests were performed at baseline; 2 weeks post-surgery and at 12 months in all IIH patients as previously described.[39] Meal stimulation testing was conducted following an overnight fast from midnight. In brief, baseline samples were collected from all patients before a standardised meal was administered (Fortisip 200ml, Cat No. 18499 309-2129, Nutricia, UK) (Composition of product found in Supplementary Table 1). A timed series of blood samples were collected at 15, 30, 60, 90 and 120 minutes following the standardised meal. Blood for gut hormones was collected in ethylenediamin tetra-acetic acid tubes (catalogue number: 456011, Greiner Bio-One Ltd, UK) containing 40 µl dipeptidyl peptidase 4 inhibitor (catalogue number: DPP4-010, Merck-Millipore UK Ltd, UK). All blood samples collected were then centrifuged (10 minutes at 1500*g* at 4°C), aliquoted as plasma in microcentrifuge tubes containing 2.5 µl protease inhibitor cocktail (catalogue number: P8340, Sigma, UK) and stored at –80°C. All samples processed only underwent a single freeze-thaw cycle.

Gut neuropeptide analysis

Active GLP-1, Ghrelin and gastric inhibitory polypeptide (GIP) plasma samples were assayed together using a customised multiplex magnetic bead-based immunoassay (MILLIPLEX® MAP Human Metabolic Hormone Magnetic Bead Panel (Catalogue # HMHEMAG-34K), Merck Millipore, Germany) according to the manufacturer's instructions and read using a Luminex MagPix® analyser. Minimum detectable concentrations were 0.4 pmol/L for active GLP-1, 3.9 pmol/L for ghrelin and 0.1 pmol/L for GIP. The precision of intra-assay and inter-assay (%CV) are <10 and <15, respectively, for all 3 assayed gut hormones.[40]

Metabolomics analysis

The detailed metabolomic analysis methods are described in the Supplementary Methods. In summary, metabolites present in plasma samples were extracted using a monophasic organic solvent (50/50 acetonitrile/water or isopropanol) and analysed by applying ultra high performance liquid chromatography-mass spectrometry assays (HILIC for water soluble metabolites and lipidomics for lipid metabolites) in positive and negative ion modes. Raw data processing was performed using XCMS. MS1, MS/MS and retention time data were applied to structurally annotate metabolites. Univariate analysis (one-way repeated measures ANOVA), spearman rank correlation analysis, hierarchical cluster analysis and pathway enrichment analysis was performed in MetaboAnalyst v5.0.

Statistical analysis

The gut neuropeptide data was analysed by calculating the total area under the curve (AUC) from fasted samples at baseline, 2 weeks post-surgery and 12-month time points as well as from the time of ingestion of the mixed meal to the postprandial phase (0 to 120 minutes) at all time points. Statistical analysis was performed using GraphPad Prism 9.4.1 9 (GraphPad software).

For the metabolomics data analysis, statistical and pathway enrichment analysis was performed in MetaboAnalyst v5.0 [41]. For statistical analysis, data were normalized to total sample response and log10 transformed. Statistical analysis applied a one-way repeated measures ANOVA, $q < 0.05$ for the baseline meal stimulated metabolite changes, over the meal stimulation test, and a two-way repeated measures ANOVA ($P < 0.005$) for metabolite time (2 weeks and 12 months) and

phenotype interactions (type of surgery). Pathway enrichment analysis applied pathway analysis, hypergeometric test (enrichment method), relative-betweenness centrality (topology analysis) and *Mus musculus* (KEGG) as the pathway library.

For the correlation analysis of ICP with metabolites we performed Spearman Rank correlation analysis. The abundance of each metabolite detected (time point 0, the start of the meal stimulation test) were correlated with ICP measured at 2 weeks post-surgery. Separately, the changes in ICP (2 weeks post-surgery minus baseline values) were also compared to changes in abundances of each metabolite detected (fasted metabolites at time point 0 of the meal stimulation test). These comparisons were performed for RYGB only patients and for the combined set of sleeve and RYGB patients. Correlation of sleeve data was not performed because data was only available for three sleeve patients.

Hierarchical Clustering Heatmaps were constructed in MetaboAnalyst using the following parameters; Features (autoscaled), distance measure (Euclidean), clustering method (Ward), samples (not clustered). The minimum or maximum peak response in comparison to the baseline sample (whichever was the higher) reported across the 120-minute period of collection post-meal were used.

Results

Patient characteristics and phenotypic changes in weight, BMI and ICP

For this study, 33 participants out of 66 recruited were randomised to a bariatric surgery, of which 27 received an intervention (Figure 1). 18 participants consented to receive a meal stimulation test (RYGB n = 7, banding n = 6, sleeve n = 5). The baseline characteristics were typical for a population of people with active IIH (Table 1).

Relationship between degree of weight loss and intracranial pressure reduction

Initially, we evaluated the degree of ICP reduction from each bariatric surgery type in relation to the amount of weight loss at 2 weeks (Table 2). The analysis at 12 months has been previously published in the entire IIH:WT study and the results pertaining to the individuals included in this study are shown in table 2.[7] We then evaluated the data at 2 weeks post-surgery. At 2 weeks, the cohort undergoing RYGB demonstrated the greatest reduction in ICP compared to other surgical types (RYGB -12.7 ± 10.5 cmCSF; gastric sleeve -6.4 ± 8.8 cmCSF; gastric banding -7.3 ± 1.1 cmCSF), with a 50 % greater reduction in RYGB compared to sleeve. This occurred despite similar weight loss in the RYGB and sleeve cohorts at 2 weeks (RYGB -10.4 ± 7.4 kg; gastric sleeve -9.9 ± 5.2 kg). The gastric banding group lost the least amount of weight at 2 weeks and had the least reduction in ICP (Table 2) (all surgeries: ΔWeight (kg) vs ΔICP (mmH_2O); r = 0.287, P = 0.263) (Supplementary Fig. 1A). At 12 months a similar but less pronounced pattern was observed with those undergoing RYGB having a 16.0 % greater reduction in ICP compared to sleeve (all surgeries: ΔWeight (kg) vs ΔICP (mmH_2O); r = 0.587, P = 0.01) (Supplementary Fig. 1B).

Gut neuropeptide meal stimulated changes

GLP-1, GIP and ghrelin were assessed over the meal stimulation protocol. In the RYGB and sleeve cohorts, the meal stimulated GLP-1 area AUC $_{0\text{ to }120}$ profile showed a marked increase following surgery (both at 2 weeks and 12 months) compared to prior to surgery, with greater increases in the RYGB vs. sleeve groups, in keeping with the literature[42, 43] (Figure 2 RYGB (A) and gastric sleeve (B)). There was a greater increase in the meal stimulated GLP-1 AUC $_{0\text{ to }120}$ profile following RYGB (434 %) (n = 7) compared to sleeve (301 %) (n = 3) at 2 weeks post-surgery. The increase was similar at 12 months between the two surgical groups (RYGB: 380% and sleeve 381%). As expected, those undergoing gastric banding (n = 5) did not show a differential meal stimulated GLP-1 AUC $_{0\text{ to }120}$ profile following surgery[43, 44] (Figure 2C). Ghrelin showed no change over the entire meal stimulated AUC $_{0\text{ to }120}$ profile (Supplementary Fig. 2A-C) in all surgery types. We would have expected to see a small decrease in ghrelin in the sleeve cohort due to the removal of the fundus of the stomach where most ghrelin-producing cells are located.[45] However, this result may be an anomaly due to low sample numbers. There was also no significant change in GIP for all surgery types over the entire meal stimulated AUC $_{0\text{ to }120}$ profile (Supplementary Fig. 2D-F), which is as expected and has been previously published.[43, 46]

Small sample sizes confounded our ability to evaluate the relationship between GLP-1 and ICP. There was a significant negative correlation (P = 0.016, r = -0.608) between GLP-1 AUC $_{0\text{ to }120}$ and absolute ICP at 12 months in those undergoing bariatric surgery (n = 15). Correlations were not observed at 2 weeks or for the change between baseline and 2 weeks.

Baseline meal stimulated metabolite changes

The dynamic changes in metabolites, over the meal stimulation test, were initially evaluated prior to bariatric surgery for meal stimulation timepoint matched patients in the IIH cohort (Supplementary Table 2). We observed dynamic changes in 150 metabolites over the course of the meal stimulation test. Perturbations of metabolites were noted over a period of 120 minutes along with alterations in lipids (acyl amino acids (eight metabolites), acyl carnitines (27 metabolites), fatty acids (13 metabolites) and oxidised fatty acids (14 metabolites)). Examples of the dynamic meal stimulated changes for acyl carnitines, fatty acids, oxidized fatty acids and triacylglycerides are shown in Figure 3.

We observed dynamic changes in vitamin A, D and E metabolites as well as nicotinamide, pantothenic acid, folic acid and iodine metabolism during the meal stimulation. It is likely that changes in these metabolites were influenced by the composition of the meal ingested (see Supplementary Table 1 for the full composition). These metabolites have not been further investigated and are not reported in Supplementary Table 2.

Early (2 week) and late (12 month) meal stimulated metabolite changes following bariatric surgery

We next compared the alteration in dynamic meal stimulated metabolites that occurred early (2 weeks; Supplementary Table 3-phenotype results) and late (12 months; Supplementary Table 4-phenotype results) after bariatric surgery in comparison to the pre-surgical meal stimulation test for all patients independent of surgery type. There were a number of similarities in metabolite

changes observed at 2 weeks and 12 months post-surgery compared to pre-surgery with glycerophospholipids being the lipid class showing the most changes at both time points. Additionally, one cholesterol esters and 4-trimethylaminobutanoate were statistically significantly altered (for direction of change see Supplementary Tables 3 and 4) both early and late after bariatric surgery. A small number of ceramides, diacylglycerides, fatty acids as well as cholesterol sulphate were statistically significantly altered at 2 weeks but not 12 months after bariatric surgery. A heirarchical clustering heatmap visualisation was used to display these differences in metabolite expression (Figure 4).

The impact of bariatric surgery type on early changes in dynamic meal stimulated metabolites

We evaluated the dynamic meal stimulated metabolite changes occurring early (2 weeks) post-surgery in comparison to pre-surgery dependent on the type of bariatric procedure (Supplementary Tables 5 (RYGB-phenotype results) and 6 (sleeve-phenotype results)). We observed metabolite changes resulting from both types of bariatric surgery (26 and 41 metabolites were statistically significantly altered (for direction of change see Supplementary Tables 5 and 6) following RYGB and sleeve interventions, respectively). Both surgical interventions resulted in statistically significant metabolite changes in glycerophospholipids; nine of 26 and 25 of 41 for RYGB and sleeve, respectively.

We further investigated the differences between RYGB and sleeve surgery at 2 weeks post-surgery via a direct statistical comparison (RYGB at 2 weeks compared to sleeve at 2 weeks; Supplementary Table 7-phenotype results). We found that there are 9 metabolites which are

statistically significant when comparing RYGB at 2 weeks and sleeve at 2 weeks and 5 of the 9 metabolites were (lyso)glycerophospholipids. Additionally, there were six metabolite changes in common at 2 weeks post-surgery for the RYGB and sleeve cohorts compared to baseline and we would suggest that these are less likely to be relevant to the increased ICP reduction in the RYGB cohort.

Glycerophospholipids and lysoglycerophospholipids show a general decrease in relative concentration at 2 weeks compared to baseline for both RYGB and sleeve groups. However, many more glycerophospholipids were perturbed in sleeve patients (25) compared to RYGB patients (9) and the magnitude of change was greater in many of these lipids in sleeve patients compared to RYGB patients (Supplementary Tables 5 and 6, Figure 4). A heirarchical clustering heatmap visualisation was used to display expression of these metabolites between RYBG (Figure 5) and sleeve (Figure 6) surgery cohorts.

The impact of bariatric surgery type on late changes in dynamic meal stimulated metabolites

We next investigated whether the dynamic metabolite changes observed during a meal stimulation test late (12 months) post-surgery in comparison to pre-surgery were dependent on the type of bariatric procedure (Supplementary Tables 8 (RYGB-phenotype results) and 9 (sleeve-phenotype results)). 55 and 11 metabolites were statistically different from pre-surgery to 12 months post-surgery for RYGB and sleeve, respectively. For RYGB, 21 of 55 statistically significant metabolites were glycerophospholipids and for sleeve six of 11 metabolites were glycerophospholipids.

We further investigated the differences between RYGB and sleeve surgery at 12 months post-surgery via a direct statistical comparison (RYGB at 12 months compared to sleeve at 12 months). 13 metabolites were statistically significant (Supplementary Table 10).

Relationship between intracranial pressure and metabolites

Next, we investigated the relationship between ICP, a measure of IIH disease activity, and metabolites. At 2 weeks post bariatric surgery we evaluated the fasted metabolites (those identified prior to the meal stimulation test) and their relationship to ICP. 75 metabolites were correlated with ICP amongst all of those participants undergoing bariatric surgery (Supplementary Table 11; the abundance of 33 metabolites were negatively correlated to ICP and the abundance of 42 metabolites were positively correlated to ICP). Of these we noted that two were ceramides, seven were glycerophospholipids (six of seven were positively correlated with ICP), seven were lysoglycerophospholipids (six of seven were positively correlated with ICP) and acetate. We then went on to evaluate the metabolites correlating with ICP at 2 weeks post-surgery in the RYGB group alone. 147 metabolite correlations were observed (Supplementary Table 12; the abundance of 57 metabolites were negatively correlated to ICP and the abundance of 90 metabolites were positively correlated to ICP). Correlations in 17 ceramides (12 were positively correlated with ICP), 32 glycerophospholipids (21 were positively correlated with ICP) and 10 lysoglycerophospholipids (seven were negatively correlated with ICP) were observed, suggesting a relationship to ICP for these lipid classes. In addition, 130 metabolites were identified as correlating with ICP in the RYGB group alone but not in the whole cohort (Supplementary Table 12B),with LysoPS (P-20:0) metabolite found to be statistically significant in both the changes in

metabolites (baseline – 2 weeks) and correlated changes in ICP (baseline – 2 weeks). These may also be of biological relevance in explaining the disproportionate reduction in ICP in the RYGB group compared to sleeve.

The smaller number of correlated ceramides and glycerophospholipids observed in the whole IIH cohort (RYGB and sleeve combined) compared to the RYGB group alone suggest that these two lipid classes are meaningfully associated with ICP in the RYGB group (as these correlations are lost when the sleeve group is combined with the RYGB group). Hence, ceramides and glycerophospholipids may be relevant to the disproportionate reduction in ICP observed in the RYGB group at 2 weeks post-surgery.

We also evaluated the relationship between changes in metabolites (between baseline and 2 weeks post-surgery) and changes in ICP in the whole bariatric cohort over this time period. 152 metabolites were correlated (Supplementary Table 13; the change in abundance of 95 metabolites were negatively correlated to the change in ICP and the change in abundance of 57 metabolites were positively correlated to the change in ICP) of which seven were ceramides, 34 glycerophospholipids and 22 lysoglycerophospholipids. However, in the RYGB cohort alone 160 metabolite changes correlated with change in ICP (the change in abundance of 96 metabolites were negatively correlated to the change in ICP and the change in abundance of 64 metabolites were positively correlated to the change in ICP). Of these 11 were ceramides, 38 glycerophospholipids and 15 lysoglycerophospholipids (Supplementary Table 14). Both glycerophospholipids and lysoglycerophospholipids were negatively correlated with ICP change and within the class of ceramide metabolites, some ceramides showed positive and some showed negative correlations

with ICP change. This suggests that these three lipid classes are associated with changes in ICP and therefore potentially important in understanding the mechanisms driving reduction in ICP following weight loss post bariatric surgery. Additionally, those correlations predominantly associated with RYGB may be relevant in explaining the exaggerated reduction in ICP amongst the RYGB cohort.

Discussion

This study sought to explore the potential mechanisms by which weight loss could exert a therapeutic effect in IIH and lower ICP. We observed rapid improvements in ICP after bariatric surgery at 2 weeks, particularly in the RYGB cohort, and hence sought to additionally explore mechanisms driving these early changes in ICP. Our data suggests that changes in GLP-1 levels and specific lipid metabolites may contribute to the reduction in ICP observed.

Role of gut neuropeptides

Very early reduction in ICP was identified at 2 weeks post-bariatric surgery. We noted that this was particularly marked amongst the group undergoing RYGB surgery (almost a two- fold greater reduction in ICP compared to the gastric sleeve cohort) despite similar reductions in weight. This was akin to what has been observed in T2D where early glycaemic control at 2 weeks post-RYGB surgery is noted in line with changes in gut neuropeptides.[32] In our cohort, at 2 weeks post-bariatric surgery the meal stimulated secretion of ghrelin and GIP showed no change, whilst meal stimulated GLP-1 secretion altered particularly in those undergoing RYGB, as has been noted in other diseases.[43, 45, 47] The greater increases in GLP-1 associated with RYGB compared to gastric sleeve

patients has been previously linked to elevated nutrient-stimulated circulating levels of GLP-1 due to increased stimulation of L cells.[43]

This was a small study which limits the interpretation of the results, however our data did suggest an association between reduction in ICP and increase in meal stimulated GLP-1 levels. This is in keeping with existing data demonstrating the importance of GLP-1 in ICP regulation in both pre-clinical and clinical data.[27, 29] The observed exaggerated reduction in ICP in the RYGB cohort could be driven by changes in GLP-1 levels following surgery, but in this small cohort further confirmatory studies are needed. GLP-1 agonist infusions have been evaluated due to their potential to replicate changes occurring after RYGB.[48] We speculate that GLP-1 agonist could have therapeutic potential in IIH in lieu of RYGB.

Lipid metabolites and ICP reduction

Comparing the untargeted metabolomics after meal stimulation testing, before and after bariatric surgery, the predominant metabolite classes to show significant dynamic changes were ceramides, glycerophospholipids and lysoglycerophospholipids. Furthermore, these lipid metabolites were associated with changes in ICP. We cannot discern a causal relationship from this data, however we would suggest that the results indicate that these lipid metabolites may have a mechanistic role in ICP reduction following weight loss. In support of this, it is known that obesity and recent weight gain are known risk factors for IIH and significant weight loss has been shown to be a disease modifying treatment of IIH.[12, 13, 49] Back translation to evaluate ceramides, glycerophospholipids and lysoglycerophospholipids in animal models of cerebrospinal fluid dynamics would be of interest.

Differential metabolite changes by surgical type

The changes in the lipid metabolites (ceramides, glycerophospholipids and lysoglycerophospholipids) were even more pronounced in those undergoing RYGB compared to sleeve (both at 2 weeks and 12 months). Additionally, there were a larger number of correlations between lipid metabolites and ICP in the RYGB cohort. Hence, changes in lipid metabolites appear to be relevant to the reduction in ICP and this relationship is amplified amongst the RYGB cohort suggesting their role is partially independent of weight loss. This is potentially relevant to understanding the exaggerated reduction of ICP in the RYGB cohort. We also note that changes in acetate correlated with ICP in this study. This is in keeping with elevated acetate levels identified in IIH compared to control subjects previously observed using nuclear magnetic resonance spectroscopy metabolite analysis.[22]

Lipid metabolites, obesity, and weight loss

The mechanisms by which ceramides, glycerophospholipids and lysoglycerophospholipids may be involved in ICP reduction following weight loss is not known. These lipid metabolite classes have been previously associated with obesity and metabolic syndrome.[50-53] Changes in these metabolites have been noted following bariatric surgery[32, 50-53] and after weight loss following lifestyle interventions,[54-58] hence are not specific to bariatric surgery but more a marker of weight loss independent of the mode of weight loss.

In IIH, HILIC-based UHPLC-MS has identified that multiple ceramides, fatty acids, glycerophospholipids and lysoglycerophospholipids are altered in association with ICP.[59] RYBG

has been previously shown to perturb ceramide levels.[32] Ceramide dysregulation has been implicated in insulin resistance and CVD risk in other diseases[9, 10, 60] and may be of relevance in IIH where an increased risk of CVD and insulin resistance has been observed.[9]

Ceramides belong to the sphingolipid family and are produced from the breakdown of membrane sphingomyelin by sphingomyelinase.[61] The brain is the organ with the highest sphingolipid content in the body.[62] Additionally, sphingomyelins are abundant in the myelin layer in the optic nerve sheath.[63, 64] The optic nerve sheath is dilated in IIH as ICP rises.[65] We hypothesize that dilation of the optic nerve sheath could lead to mechanical stress and sphingomyelin breakdown and production of ceramide. Hence ceramide could reflect a biomarker of elevated ICP in IIH. It is interesting to note that changes in the brain's lipid levels, including glycerophospholipids,[66] are associated with other pathogenic processes including neuroinflammatory diseases such as Alzheimer's disease and Parkinson's disease.[67-69] Future work to explore the impact of lipid metabolites on ICP regulation would be of interest.

Limitations

There are some limitations to the reported study which should be considered. Due to the rarity of the disease, there were relatively small numbers of participants in the surgery cohorts. However, this was the first study to explore the changes of metabolites following bariatric surgery in IIH patients and this sample size is larger compared to other IIH studies. In addition, the small sample size may have limited the ability to discern charges in some metabolites and gut neuro-peptides. For example existing literature suggest that ghrelin alters after sleeve gastrectomy, but in this small study we did not observe this change. Untargeted UHPLC-MS metabolomics is not able to quantify

metabolite changes, but this would be of future interest. UHPLC-MS does however, have the advantage of being untargeted and hence our findings reflect a broad discovery based approach. We have not evaluated the functional significance of our findings currently, but this study guides future research work. It is not possible to say if changes in lipid metabolites are a cause or consequence of ICP changes until further functional evaluations are conducted. There was no non-IIH cohort, in which meal stimulated samples were collected (as this work has previously been conducted).[32] However, the aim of this study was not to determine if metabolite changes after bariatric surgery were unique to IIH, but to determine how metabolite changes in IIH related to changes in ICP. Metabolites were sought in plasma, however it would be a future interest to analyse the changes in metabolite signatures in the CSF following bariatric surgery.

Some metabolites are identified based on comparison of retention time and/or MS/MS data to data collected for authentic chemical standards, though other metabolites are annotated without comparison to chemical standards. For this reason, we have applied pathway enrichment analysis to reduce (but not fully eliminate) the probability of false positive conclusions. For example, if eight metabolites are statistically significant and present in a single pathway then we have more confidence that this is a biologically valid conclusion compared to deriving biological conclusions from a single statistically significant metabolite without applying pathway enrichment analysis.

Conclusion

Reduction in weight, driven by bariatric surgery, both early (2 weeks) and late (12 months), was associated with novel changes in lipid metabolism (notably ceramides, glycerophospholipids and lysoglycerphospholipids) which correlated with changes in ICP. We observed rapid improvements

in ICP at 2 weeks post-bariatric surgery, particularly in the RYGB group, despite similar degrees of weight loss in the other surgical types. At 2 weeks post-surgery, changes in lipid metabolism and GLP-1 levels were of greater magnitude in the RYGB group, potentially indicating their importance in driving the exaggerated ICP reduction in this surgical type. Ceramides, glycerophospholipids and lysoglycerphospholipids were strongly associated with changes in ICP at 2 weeks post-surgery in the RYGB cohort (Figure 7). The mechanisms by which changes in lipid metabolites influence ICP are yet to be explored. We suggest that these novel perturbations in lipid metabolism and GLP-1 secretion are mechanistically important in driving reduction in ICP following weight loss in patients with IIH. However, the small sample size precludes firm conclusions being drawn. Therapeutic targeting however, of these pathways, for example with GLP-1 agonist administration, could represent a therapeutic strategy.

Data availability statement

The authors confirm that the data supporting the findings of this study are available within the article and its supplementary material.

Funding

ZA was funded by the Lundbeck foundation. AY is funded by the Association of British Neurologists and Guarantors of the Brain Clinical Research Training Fellowship. OG is funded by a Brain Research UK PhD studentship. AJS was funded by a National Institute for Health and Care Research (NIHR) clinician scientist fellowship (NIHR-CS-011-028) and the Medical Research Council (MRC), UK (MR/K015184/1ii) for the duration of the study. AJS is funded by a Sir Jules Thorn Award for Biomedical Science. The views expressed are those of the authors and not

necessarily those of the UK National Health Service, the National Institute for Health and Care Research, or the UK department of Health and Social Care.

Role of Funder/Sponsor

The funders had no role in the design or conduct of the study; no role in collection, management, analysis, or interpretation of the data; preparation, review, or approval of the manuscript; and no role in the decision to submit the manuscript for publication.

Competing Interests

SPM reports consultancy fees and advisory boards from Invex Therapeutics, educational fees from Heidelberg engineering during the conduct of the study; outside the submitted work she has received Honoria for education and advisory boards from Chugai-Roche Ltd, Gensight, Janssen, Allergan, Santen, Teva, Roche, and Neurodiem. OG reports scientific consultancy fees from Invex therapeutics during the conduct of the study, outside the submitted work. AY reports receiving speaker fees for educational talk from Teva, UK outside the submitted work. AJS reports consulting fees and stockholding with Invex therapeutics, during the conduct of the study, outside of the submitted work she has received honoraria for education and advisory boards from Allergan, Amgen, Novartis and Cheisi outside the submitted work. AAT reports grants from Novo Nordisk, personal fees from Novo Nordisk, non-financial support from Novo Nordisk, personal fees from Eli Lilly, non-financial support from Eli Lilly, personal fees from Janssen, personal fees from AZ, non-financial support from AZ, non-financial support from Impeto medical, non-financial support from Resmed, non-financial support from Aptiva, personal fees from BI, non-financial support from BI, personal fees from BMS, nonfinancial support from BMS, personal fees from NAPP,

non-financial support from NAPP, personal fees from MSD, non-financial support from MSD, personal fees from Nestle, personal fees from Gilead, grants from Sanofi, and personal fees from Sanofi outside the submitted work. AAT is currently an employee of Novo Nordisk. Novo Nordisk had no role in this project. All other authors declare no competing interests.

Supplementary material

Supplementary material is available at *Brain Communications* online.

References

1. Mollan SP, Sinclair AJ. Outcomes measures in idiopathic intracranial hypertension. Expert Rev Neurother. 2021;21(6):687-700.
2. Thaller M, Homer V, Hyder Y, et al. The idiopathic intracranial hypertension prospective cohort study: evaluation of prognostic factors and outcomes. J Neurol. 2022.
3. Corbett JJ, Savino PJ, Thompson HS, et al. Visual loss in pseudotumor cerebri. Follow-up of 57 patients from five to 41 years and a profile of 14 patients with permanent severe visual loss. Arch Neurol. 1982;39(8):461-74.
4. Mollan SP, Grech O, Sinclair AJ. Headache attributed to idiopathic intracranial hypertension and persistent post-idiopathic intracranial hypertension headache: A narrative review. Headache. 2021;61(6):808-16.
5. Mollan SP, Wakerley BR, Alimajstorovic Z, et al. Intracranial pressure directly predicts headache morbidity in idiopathic intracranial hypertension. J Headache Pain. 2021;22(1):118.
6. Virdee J, Larcombe S, Vijay V, et al. Reviewing the Recent Developments in Idiopathic Intracranial Hypertension. Ophthalmol Ther. 2020;9(4):767-81.
7. Mollan SP, Tahrani AA, Sinclair AJ. The Potentially Modifiable Risk Factor in Idiopathic Intracranial Hypertension: Body Weight. Neurol Clin Pract. 2021;11(4):e504-e7.
8. Mollan SP, Aguiar M, Evison F, Frew E, Sinclair AJ. The expanding burden of idiopathic intracranial hypertension. Eye (Lond). 2019;33(3):478-85.
9. Adderley NJ, Subramanian A, Nirantharakumar K, et al. Association Between Idiopathic Intracranial Hypertension and Risk of Cardiovascular Diseases in Women in the United Kingdom. JAMA Neurol. 2019;76(9):1088-98.
10. Westgate CS, Botfield HF, Alimajstorovic Z, et al. Systemic and adipocyte transcriptional and metabolic dysregulation in idiopathic intracranial hypertension. JCI Insight. 2021;6(10).
11. Hornby C, Botfield H, O'Reilly MW, et al. Evaluating the Fat Distribution in Idiopathic Intracranial Hypertension Using Dual-Energy X-ray Absorptiometry Scanning. Neuroophthalmology. 2018;42(2):99-104.

12. Mollan SP, Mitchell JL, Ottridge RS, et al. Effectiveness of Bariatric Surgery vs Community Weight Management Intervention for the Treatment of Idiopathic Intracranial Hypertension: A Randomized Clinical Trial. JAMA Neurol. 2021;78(6):678-86.
13. Sinclair AJ, Burdon MA, Nightingale PG, et al. Low energy diet and intracranial pressure in women with idiopathic intracranial hypertension: prospective cohort study. BMJ. 2010;341:c2701.
14. Yiangou A, Mitchell JL, Nicholls M, et al. Obstructive sleep apnoea in women with idiopathic intracranial hypertension: a sub-study of the idiopathic intracranial hypertension weight randomised controlled trial (IIH: WT). J Neurol. 2022;269(4):1945-56.
15. Westgate CSJ, Markey K, Mitchell JL, et al. Increased systemic and adipose 11β-HSD1 activity in idiopathic intracranial hypertension. Eur J Endocrinol. 2022;187(2):323-33.
16. O'Reilly MW, Westgate CS, Hornby C, et al. A unique androgen excess signature in idiopathic intracranial hypertension is linked to cerebrospinal fluid dynamics. JCI Insight. 2019;4(6).
17. Hardy RS, Botfield H, Markey K, et al. 11βHSD1 Inhibition with AZD4017 Improves Lipid Profiles and Lean Muscle Mass in Idiopathic Intracranial Hypertension. J Clin Endocrinol Metab. 2021;106(1):174-87.
18. Thaller M, Mytton J, Wakerley BR, Mollan SP, Sinclair AJ. Idiopathic intracranial hypertension: Evaluation of births and fertility through the Hospital Episode Statistics dataset. BJOG. 2022.
19. Thaller M, Wakerley BR, Abbott S, et al. Managing idiopathic intracranial hypertension in pregnancy: practical advice. Pract Neurol. 2022;22(4):295-300.
20. Grech O, Mollan SP, Wakerley BR, et al. The Role of Metabolism in Migraine Pathophysiology and Susceptibility. Life (Basel). 2021;11(5).
21. Grech O, Sassani M, Terwindt G, et al. Alterations in metabolic flux in migraine and the translational relevance. J Headache Pain. 2022;23(1):127.
22. Grech O, Seneviratne SY, Alimajstorovic Z, et al. Nuclear Magnetic Resonance Spectroscopy Metabolomics in Idiopathic Intracranial Hypertension to Identify Markers of Disease and Headache. Neurology. 2022.
23. Vilsbøll T, Christensen M, Junker AE, Knop FK, Gluud LL. Effects of glucagon-like peptide-1 receptor agonists on weight loss: systematic review and meta-analyses of randomised controlled trials. BMJ. 2012;344:d7771.
24. Campbell JE, Drucker DJ. Pharmacology, physiology, and mechanisms of incretin hormone action. Cell Metab. 2013;17(6):819-37.
25. Larsen PJ, Tang-Christensen M, Holst JJ, Orskov C. Distribution of glucagon-like peptide-1 and other preproglucagon-derived peptides in the rat hypothalamus and brainstem. Neuroscience. 1997;77(1):257-70.
26. Astrup A, Rössner S, Van Gaal L, et al. Effects of liraglutide in the treatment of obesity: a randomised, double-blind, placebo-controlled study. Lancet. 2009;374(9701):1606-16.
27. Botfield HF, Uldall MS, Westgate CSJ, et al. A glucagon-like peptide-1 receptor agonist reduces intracranial pressure in a rat model of hydrocephalus. Sci Transl Med. 2017;9(404).
28. Ast J, Arvaniti A, Fine NHF, et al. Super-resolution microscopy compatible fluorescent probes reveal endogenous glucagon-like peptide-1 receptor distribution and dynamics. Nat Commun. 2020;11(1):467.
29. Mitchell JL, Lyons HS, Walker JK, et al. The effect of GLP-1RA exenatide on Idiopathic Intracranial Hypertension: Randomised Clinical Trial. medRxiv. 2022:2022.05.24.22275518.

30. Mollan SP, Mitchell JL, Yiangou A, et al. Association of Amount of Weight Lost After Bariatric Surgery With Intracranial Pressure in Women With Idiopathic Intracranial Hypertension. Neurology. 2022;99(11):e1090-e9.
31. Behary P, Tharakan G, Alexiadou K, et al. Combined GLP-1, Oxyntomodulin, and Peptide YY Improves Body Weight and Glycemia in Obesity and Prediabetes/Type 2 Diabetes: A Randomized, Single-Blinded, Placebo-Controlled Study. Diabetes Care. 2019;42(8):1446-53.
32. Jones B, Sands C, Alexiadou K, et al. The Metabolomic Effects of Tripeptide Gut Hormone Infusion Compared to Roux-en-Y Gastric Bypass and Caloric Restriction. J Clin Endocrinol Metab. 2022;107(2):e767-e82.
33. Sudlow A, le Roux CW, Pournaras DJ. Review of multimodal treatment for type 2 diabetes: combining metabolic surgery and pharmacotherapy. Ther Adv Endocrinol Metab. 2019;10:2042018819875407.
34. Abdeen G, le Roux CW. Mechanism Underlying the Weight Loss and Complications of Roux-en-Y Gastric Bypass. Review. Obes Surg. 2016;26(2):410-21.
35. Ottridge R, Mollan SP, Botfield H, et al. Randomised controlled trial of bariatric surgery versus a community weight loss programme for the sustained treatment of idiopathic intracranial hypertension: the Idiopathic Intracranial Hypertension Weight Trial (IIH:WT) protocol. BMJ Open. 2017;7(9):e017426.
36. Elliot L, Frew E, Mollan SP, et al. Cost-effectiveness of bariatric surgery versus community weight management to treat obesity-related idiopathic intracranial hypertension: evidence from a single-payer healthcare system. Surg Obes Relat Dis. 2021;17(7):1310-6.
37. Khoury JM, Donahue SP, Lavin PJ, Tsai JC. Comparison of 24-2 and 30-2 perimetry in glaucomatous and nonglaucomatous optic neuropathies. J Neuroophthalmol. 1999;19(2):100-8.
38. Vijay V, Mollan SP, Mitchell JL, et al. Using Optical Coherence Tomography as a Surrogate of Measurements of Intracranial Pressure in Idiopathic Intracranial Hypertension. JAMA Ophthalmol. 2020;138(12):1264-71.
39. le Roux CW, Aylwin SJ, Batterham RL, et al. Gut hormone profiles following bariatric surgery favor an anorectic state, facilitate weight loss, and improve metabolic parameters. Ann Surg. 2006;243(1):108-14.
40. McGlone ER, Malallah K, Cuenco J, et al. Differential effects of bile acids on the postprandial secretion of gut hormones: a randomized crossover study. Am J Physiol Endocrinol Metab. 2021;320(4):E671-E9.
41. Pang Z, Chong J, Zhou G, et al. MetaboAnalyst 5.0: narrowing the gap between raw spectra and functional insights. Nucleic Acids Res. 2021;49(W1):W388-W96.
42. Dirksen C, Jørgensen NB, Bojsen-Møller KN, et al. Gut hormones, early dumping and resting energy expenditure in patients with good and poor weight loss response after Roux-en-Y gastric bypass. Int J Obes (Lond). 2013;37(11):1452-9.
43. Pucci A, Batterham RL. Mechanisms underlying the weight loss effects of RYGB and SG: similar, yet different. J Endocrinol Invest. 2019;42(2):117-28.
44. Cummings DE, Weigle DS, Frayo RS, et al. Plasma ghrelin levels after diet-induced weight loss or gastric bypass surgery. N Engl J Med. 2002;346(21):1623-30.
45. Yousseif A, Emmanuel J, Karra E, et al. Differential effects of laparoscopic sleeve gastrectomy and laparoscopic gastric bypass on appetite, circulating acyl-ghrelin, peptide YY3-36 and active GLP-1 levels in non-diabetic humans. Obes Surg. 2014;24(2):241-52.

46. Alexiadou K, Cuenco J, Howard J, et al. Proglucagon peptide secretion profiles in type 2 diabetes before and after bariatric surgery: 1-year prospective study. BMJ Open Diabetes Res Care. 2020;8(1).
47. Dar MS, Chapman WH, 3rd, Pender JR, et al. GLP-1 response to a mixed meal: what happens 10 years after Roux-en-Y gastric bypass (RYGB)? Obes Surg. 2012;22(7):1077-83.
48. Hutch CR, Sandoval D. The Role of GLP-1 in the Metabolic Success of Bariatric Surgery. Endocrinology. 2017;158(12):4139-51.
49. Mollan SP, Davies B, Silver NC, et al. Idiopathic intracranial hypertension: consensus guidelines on management. J Neurol Neurosurg Psychiatry. 2018;89(10):1088-100.
50. Kang M, Yoo HJ, Kim M, Kim M, Lee JH. Metabolomics identifies increases in the acylcarnitine profiles in the plasma of overweight subjects in response to mild weight loss: a randomized, controlled design study. Lipids Health Dis. 2018;17(1):237.
51. Perng W, Rifas-Shiman SL, Sordillo J, Hivert MF, Oken E. Metabolomic Profiles of Overweight/Obesity Phenotypes During Adolescence: A Cross-Sectional Study in Project Viva. Obesity (Silver Spring). 2020;28(2):379-87.
52. Monnerie S, Comte B, Ziegler D, et al. Metabolomic and Lipidomic Signatures of Metabolic Syndrome and its Physiological Components in Adults: A Systematic Review. Scientific Reports. 2020;10(1):669.
53. Yin X, Willinger CM, Keefe J, et al. Lipidomic profiling identifies signatures of metabolic risk. EBioMedicine. 2020;51:102520.
54. Schenk S, Horowitz JF. Acute exercise increases triglyceride synthesis in skeletal muscle and prevents fatty acid-induced insulin resistance. J Clin Invest. 2007;117(6):1690-8.
55. Dubé JJ, Amati F, Stefanovic-Racic M, et al. Exercise-induced alterations in intramyocellular lipids and insulin resistance: the athlete's paradox revisited. Am J Physiol Endocrinol Metab. 2008;294(5):E882-8.
56. Dubé JJ, Amati F, Toledo FG, et al. Effects of weight loss and exercise on insulin resistance, and intramyocellular triacylglycerol, diacylglycerol and ceramide. Diabetologia. 2011;54(5):1147-56.
57. Andersson A, Sjödin A, Olsson R, Vessby B. Effects of physical exercise on phospholipid fatty acid composition in skeletal muscle. Am J Physiol. 1998;274(3):E432-8.
58. San Martin R, Brandao CFC, Junqueira-Franco MVM, et al. Untargeted lipidomic analysis of plasma from obese women submitted to combined physical exercise. Sci Rep. 2022;12(1):11541.
59. Alimajstorovic Z, Mollan SP, Grech O, et al. Dysregulation of Amino Acid, Lipid, and Acylpyruvate Metabolism in Idiopathic Intracranial Hypertension: A Non-targeted Case Control and Longitudinal Metabolomic Study. J Proteome Res. 2022.
60. Field BC, Gordillo R, Scherer PE. The Role of Ceramides in Diabetes and Cardiovascular Disease Regulation of Ceramides by Adipokines. Front Endocrinol (Lausanne). 2020;11:569250.
61. Lee JY, Jin HK, Bae JS. Sphingolipids in neuroinflammation: a potential target for diagnosis and therapy. BMB Rep. 2020;53(1):28-34.
62. Kosicek M, Hecimovic S. Phospholipids and Alzheimer's disease: alterations, mechanisms and potential biomarkers. Int J Mol Sci. 2013;14(1):1310-22.
63. Giussani P, Prinetti A, Tringali C. The role of Sphingolipids in myelination and myelin stability and their involvement in childhood and adult demyelinating disorders. J Neurochem. 2021;156(4):403-14.

64. Wattenberg BW. Intra- and intercellular trafficking in sphingolipid metabolism in myelination. Adv Biol Regul. 2019;71:97-103.
65. Watanabe A, Kinouchi H, Horikoshi T, Uchida M, Ishigame K. Effect of intracranial pressure on the diameter of the optic nerve sheath. J Neurosurg. 2008;109(2):255-8.
66. Fonteh AN, Chiang J, Cipolla M, et al. Alterations in cerebrospinal fluid glycerophospholipids and phospholipase A2 activity in Alzheimer's disease. J Lipid Res. 2013;54(10):2884-97.
67. Assi E, Cazzato D, De Palma C, et al. Sphingolipids and brain resident macrophages in neuroinflammation: an emerging aspect of nervous system pathology. Clin Dev Immunol. 2013;2013:309302.
68. Liu Q, Zhang J. Lipid metabolism in Alzheimer's disease. Neurosci Bull. 2014;30(2):331-45.
69. Yin F, Sancheti H, Patil I, Cadenas E. Energy metabolism and inflammation in brain aging and Alzheimer's disease. Free Radic Biol Med. 2016;100:108-22.

Figure legends

Figure 1 Consort diagram. 33 participants out of 66 recruited were randomised to a bariatric surgery, of which 27 received an intervention. All 18 participants were female and consented to receive a meal stimulation test (RYGB n = 7, banding n = 6, sleeve n = 5). *RYGB, Roux-En-Y gastric bypass.*

Figure 2 GLP-1 gut hormone responses in all surgical cohorts at all time points. Total area under the curve dynamics of GLP-1 RYGB (Baseline Total Area: 1240±490.6; 2 Weeks Total Area: 6623±688.4, +434%; 12 Months Total Area: 5947±1222, +380%) (n = 7) (A); gastric sleeve (Baseline Total Area: 1045±253.1; 2 Weeks Total Area: 4194±810.8, +301%; 12 Months Total Area: 5029±973.3, +381%) (n = 3) (B); gastric banding (Baseline Total Area: 332.7±124.0; 2 Weeks Total Area: 626.4±184.8, +88%; 12 Months Total Area: 527.3±143.9, +59%) (n = 5) (C) following a meal stimulation at 0 to 120 minutes as total area ± standard error, and percentage change over baseline. Only descriptive analysis was performed on this figure. No formal statistical testing was performed. Total Area units = (pmol/l x minutes). Baseline: black lines; 2 weeks post-

surgery: red lines; 12 months post-surgery: blue lines. *GLP-1, glucagon-like peptide-1; RYGB, Roux-En-Y gastric bypass.*

Figure 3 Box and whisker plots demonstrate changes over time for specific lipid classes. Total area under the curve as a normalised response % of Docosahexaenoic acid (Total Area: 4.943±0.5455) (A); hydroxy-hexadecanoic acid (Total Area: 1.794±0.05924) (B); tetradecadiencarnitine (Total Area: 6.072±0.5966) (C); TG(56:3) (Total Area: 0.6301±0.6480) (D) at each time point (0, 15, 30, 60, 90, 120 minutes) at baseline which is composed of timepoint matched IIH subjects prior to surgery (n = 6) as total area ± standard error. A one-way repeated measures ANOVA was applied with correction applied for multiple testing (Benjamini-Hochberg method) with a q-value<0.05 to find the significant metabolite expression from the samples. Only descriptive analysis was performed on this figure. No formal statistical testing was performed.

Figure 4 Hierarchical clustering heatmap visualizing data for all IIH subjects (bypass and sleeve). Hierarchical Clustering Heatmaps were constructed in MetaboAnalyst using the following parameters; features (autoscaled), distance measure (Euclidean), clustering method (Ward), samples (not clustered). A subset of lipids with q<0.05 were chosen to visualise trends in the data. Baseline (magenta), 2-weeks post-surgery (green) and 12 months post-surgery (blue). All statistically significant metabolites for the comparison of baseline vs. 2-weeks or baseline vs. 12 months are included. Blue are low abundances and red are high abundances. (n = 12). *AC, acyl carnitine; GPL, glycerophospholipid; TG, triacylglyceride; MC, mixed class; CER, ceramide; LGPL, lysoglycerophospholipid; OC, other class; DG, diacyglyceride; CDP, glycerol; FA, fatty acid; OFA, oxidized fatty acid.*

Figure 5 Hierarchical clustering heatmap visualizing data for all bypass subjects. Hierarchical Clustering Heatmaps were constructed in MetaboAnalyst using the following parameters; features (autoscaled), distance measure (Euclidean), clustering method (Ward), samples (not clustered). A subset of lipids with q<0.05 were chosen to visualise trends in the data. Baseline (red) and 2-weeks post-surgery (green). All statistically significant metabolites for the comparison of baseline vs. 2-weeks are included. Blue are low abundances and red are high abundances. Bypass (n = 7). *AC, acyl carnitine; GPL, glycerophospholipid; TG, triacylglyceride; MC, mixed class; LGPL, lysoglycerophospholipid; OC, other class; H, heme; AAA, acyl amino acid; CER, ceramide; OFA, oxidized fatty acid.*

Figure 6 Hierarchical clustering heatmap visualizing data for all sleeve subjects. Hierarchical Clustering Heatmaps were constructed in MetaboAnalyst using the following parameters; features (autoscaled), distance measure (Euclidean), clustering method (Ward), samples (not clustered). A subset of lipids with q<0.05 were chosen to visualise trends in the data. Baseline (red) and 2-weeks post-surgery (green). All statistically significant metabolites for the comparison of baseline vs. 2-weeks are included. Blue are low abundances and red are high abundances. Sleeve (n = 5). *AC, acyl carnitine; GPL, glycerophospholipid; TG, triacylglyceride; MC, mixed class; LGPL, lysoglycerophospholipid; OC, other class; H, heme; AAA, acyl amino acid; CER, ceramide; OFA, oxidized fatty acid.*

Figure 7 Infographic. In idiopathic intracranial hypertension, novel changes were noticed in lipid metabolites (glycerphospholipids, lysoglycerphospholipids and ceramides) and meal stimulated glucagon-like peptide-1 levels, in patients following Roux-En-Y gastric bypass surgery, which

were associated with changes in intracranial pressure. 19 and 20 different metabolites were perturbed between the RYGB and sleeve cohorts at 2 weeks and 12 months post surgery, respectively. *GLP-1, glucagon-like peptide-1; ICP, intracranial pressure.*

Table 1 Baseline characteristics of study subject combined and split by surgery type (RYGB, sleeve and band)

Baseline Characteristics	All surgeries (*n* = 18)	RYGB (*n* = 7)	Sleeve (*n* = 5)	Band (*n* = 6)
Age (years)	30.8 (6.9)	32.7 (9.2)	29.4 (6.9)	29.8 (4.0)
Weight (kg)	111.9 (20.4)	115.0 (27.3)	113.1 (19.8)	107.2 (13.0)
BMI (kg/m²)	42.9 (7.0)	45.5 (9.6)	42.2 (4.3)	40.4 (4.8)
Intracranial Pressure (cmCSF)	35.6 (4.5)	35.6 (5.6)	35.6 (4.7)	35.5 (3.6)
Systolic Blood Pressure (mmHg)	124.8 (18.4)	131.8 (17.3)	126.2 (10.4)	115.4 (23.1)
Perimetric mean deviation (worst eye) (dB)	-4.3 (3.9)	-4.0 (3.9)	-4.8 (6.0)	-4.4 (1.1)
Papilloedema measured by OCT global RNFL (worst eye) (µm)	160.1 (128.3)	196.6 (191.4)	136.0 (61.8)	133.0 (55.3)
Monthly Headache Days	23.6 (6.6)	24.6 (5.9)	21.6 (8.3)	24.0 (6.7)
Frisén Grading of Papilloedema (worst eye)	2.2 (1.0)	2.3 (1.0)	2.5 (1.0)	1.8 (1.3)

Data presented as mean ± SD. *n*, Number; *BMI, Body Mass Index; CSF, cerebrospinal fluid; OCT, optical coherence tomography; RNFL, retinal nerve fibre layer; RYGB, Roux-En-Y gastric bypass; SD, standard deviation.*

Table 2 Absolute and delta change (Δ) values for age, BMI, ICP and weight

	Baseline Mean (SD)				2 weeks post-surgery Mean (SD)				12 Months Mean (SD)			
	All surgeries (*n* = 18)	RYGB (*n* = 7)	Sleeve (*n* = 5)	Band (*n* = 6)	All surgeries (*n* = 18)	RYGB (*n* = 7)	Sleeve (*n* = 5)	Band (*n* = 6)	All surgeries (*n* = 18)	RYGB (*n* = 7)	Sleeve (*n* = 5)	Band (*n* = 6)
Age (years)	30.8 (6.9)	32.7 (9.2)	29.4 (6.9)	29.8 (4.0)								
BMI (kg/m²)	42.9 (7.0)	45.5 (9.6)	42.2 (4.3)	40.4 (4.8)	38.7 (6.3)	40.2 (8.6)	37.9 (5.3)	37.6 (4.2)	32.8 (6.8)	32.3 (9.8)	31.0 (3.6)	34.9 (4.8)
BMI Δ change					-3.9 (2.2)	-4.3 (3.0)	-4.4 (2.1)	-2.9 (1.3)	-9.8 (4.7)	-12.2 (4.0)	-11.28 (4.5)	-6.1 (3.0)
Weight (kg)	111.9 (20.4)	115.0 (27.3)	113.1 (19.8)	107.2 (13.0)	102.3 (18.8)	104.6 (24.0)	103.2 (21.0)	98.9 (11.7)	86.0 (19.8)	83.0 (27.0)	82.2 (13.6)	92.7 (15.3)
Weight Δ change					-9.6 (5.4)	-10.4 (7.4)	-9.9 (5.2)	-8.4 (2.8)	-25.9 (11.9)	-32.0 (8.0)	-30.9 (12.6)	-14.6 (7.1)
ICP (cmCSF)	35.6 (4.5)	35.6 (5.6)	35.6 (4.7)	35.5 (3.6)	26.9 (8.1)	23.9 (6.8)	29.2 (12.2)	28.1 (3.8)	22.7 (5.4)	19.6 (4.4)	22.1 (6.1)	26.9 (3.1)
ICP Δ change					-9.0 (8.11)	-12.7 (10.5)	-6.4 (8.8)	-7.3 (1.3)	-12.9 (7.2)	-16.1 (8.4)	-13.5 (8.0)	-7.4 (3.9)

Baseline, 2 weeks post-surgery and 12 month time points for grouped and split by surgery types (RYGB, sleeve and band).

Data presented as mean ± SD. *n*, Number; *BMI, Body Mass Index; ICP, intracranial pressure; RYGB, Roux-En-Y gastric bypass.*

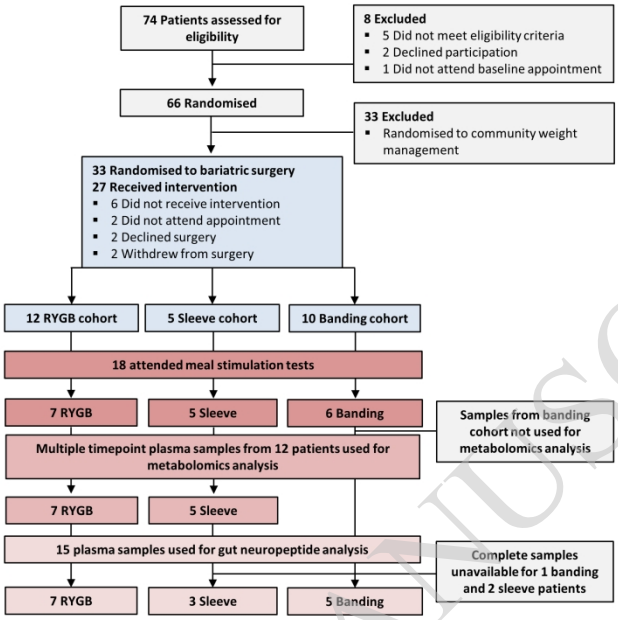

Figure 1

254x190mm (300 x 300 DPI)

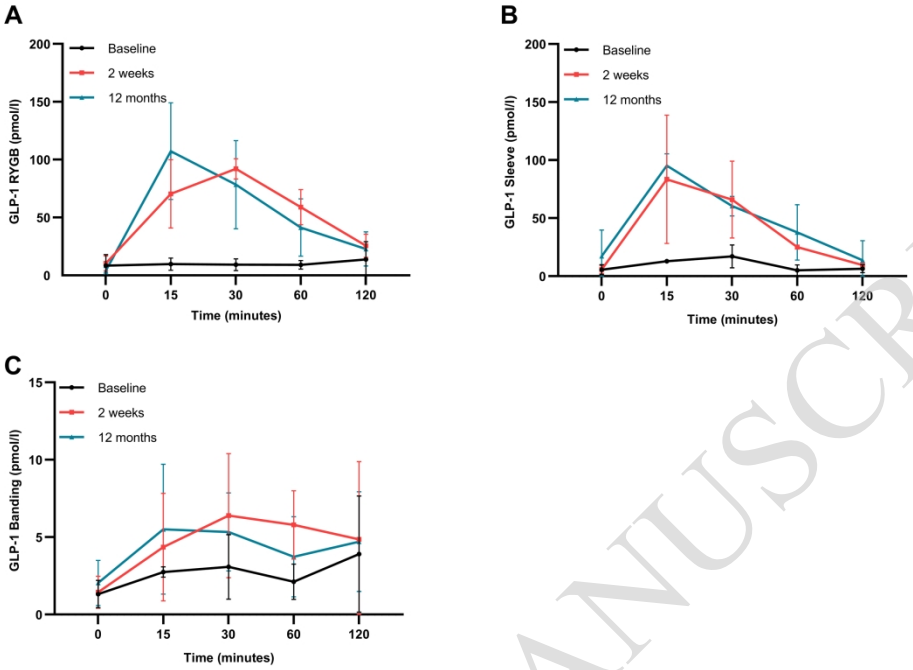

Figure 2

276x195mm (300 x 300 DPI)

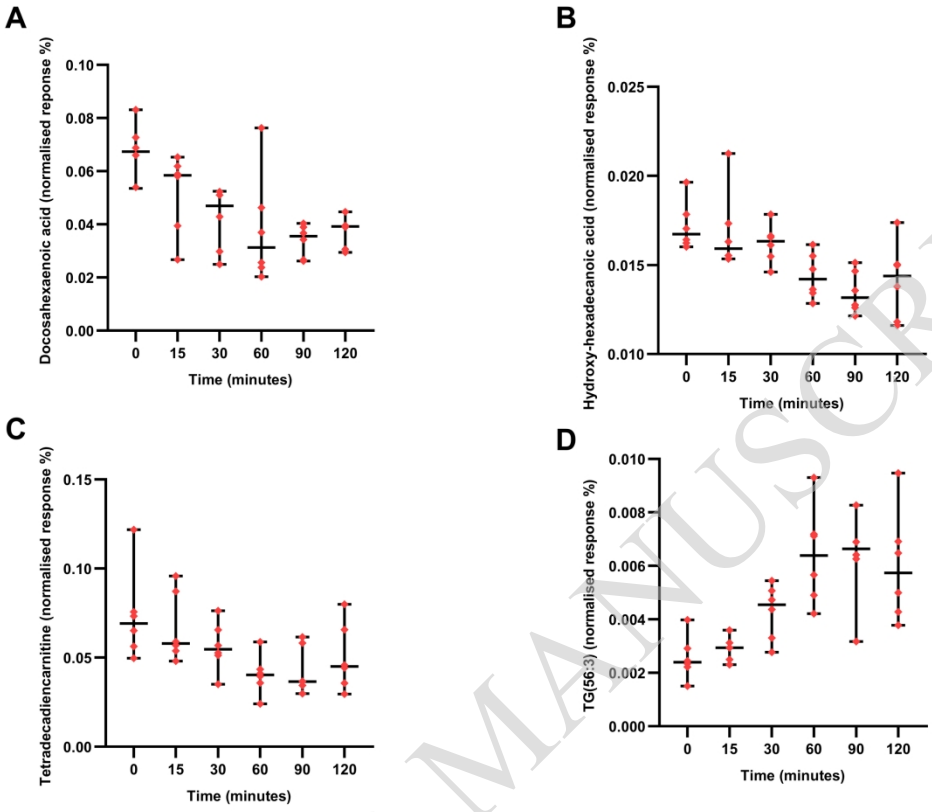

Figure 3

235x201mm (300 x 300 DPI)

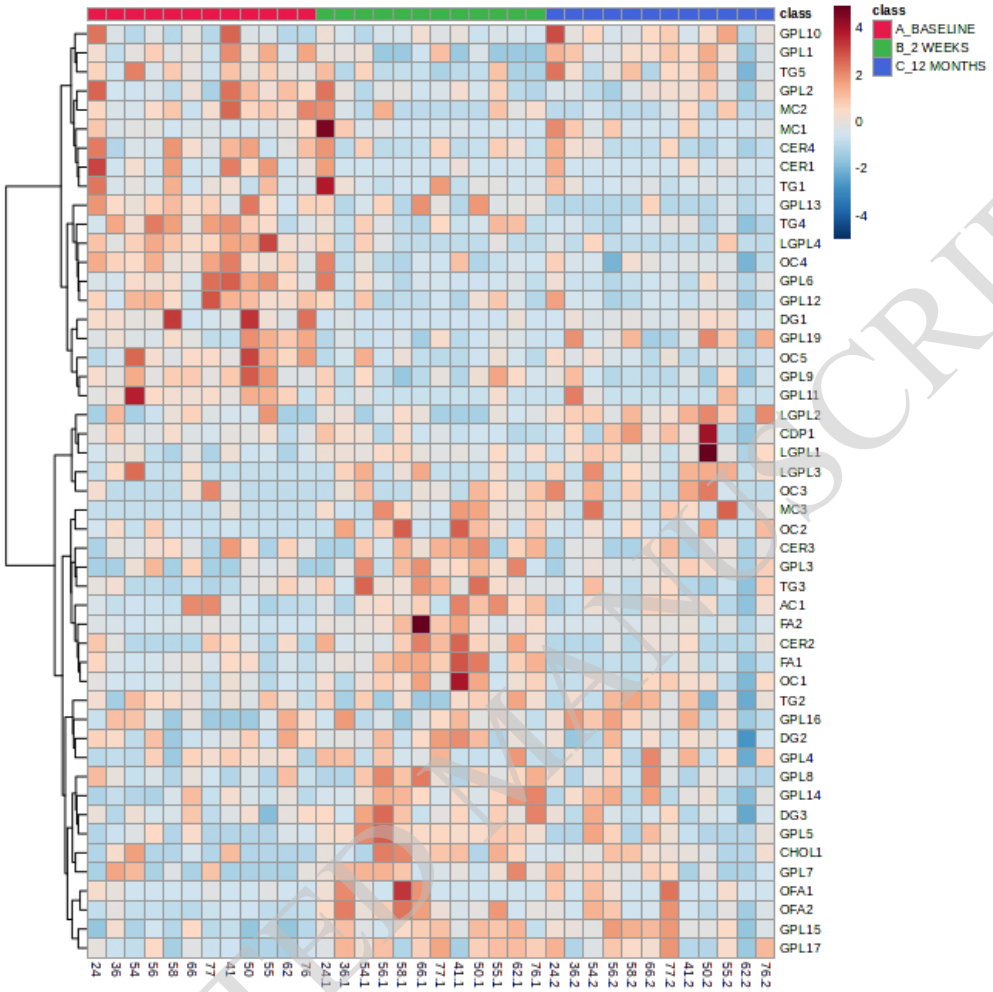

Figure 4

228x228mm (72 x 72 DPI)

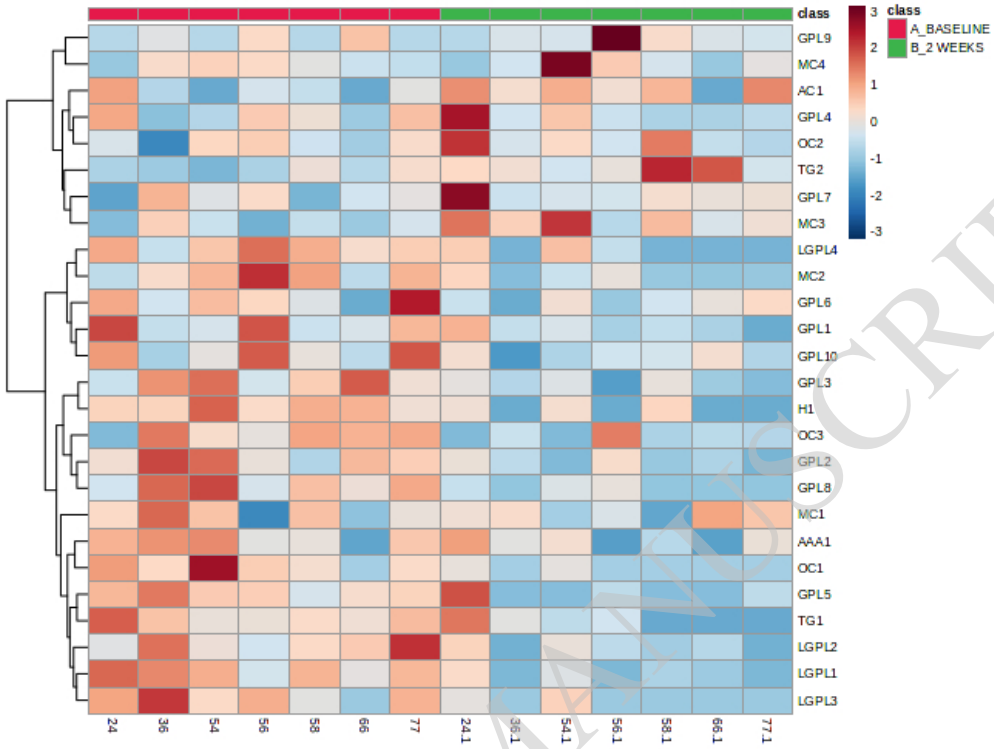

Figure 5

228x172mm (72 x 72 DPI)

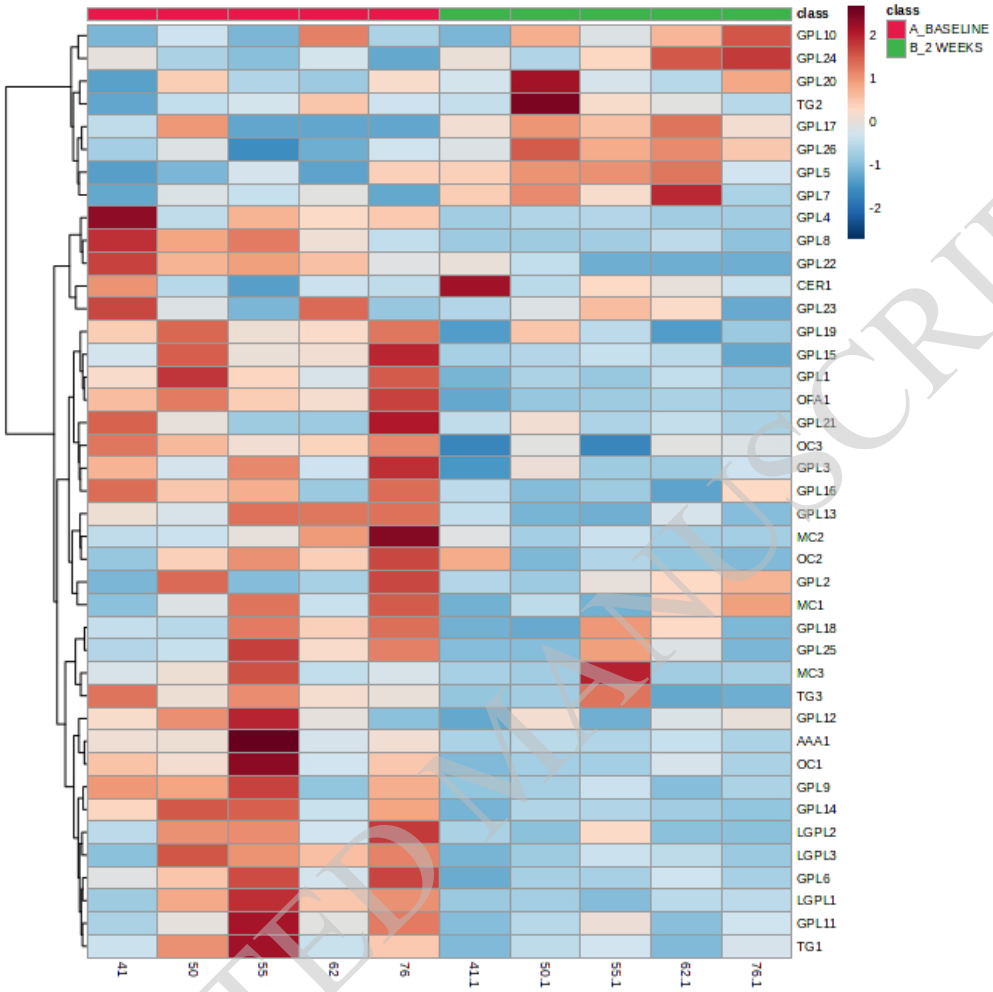

Figure 6

228x228mm (72 x 72 DPI)

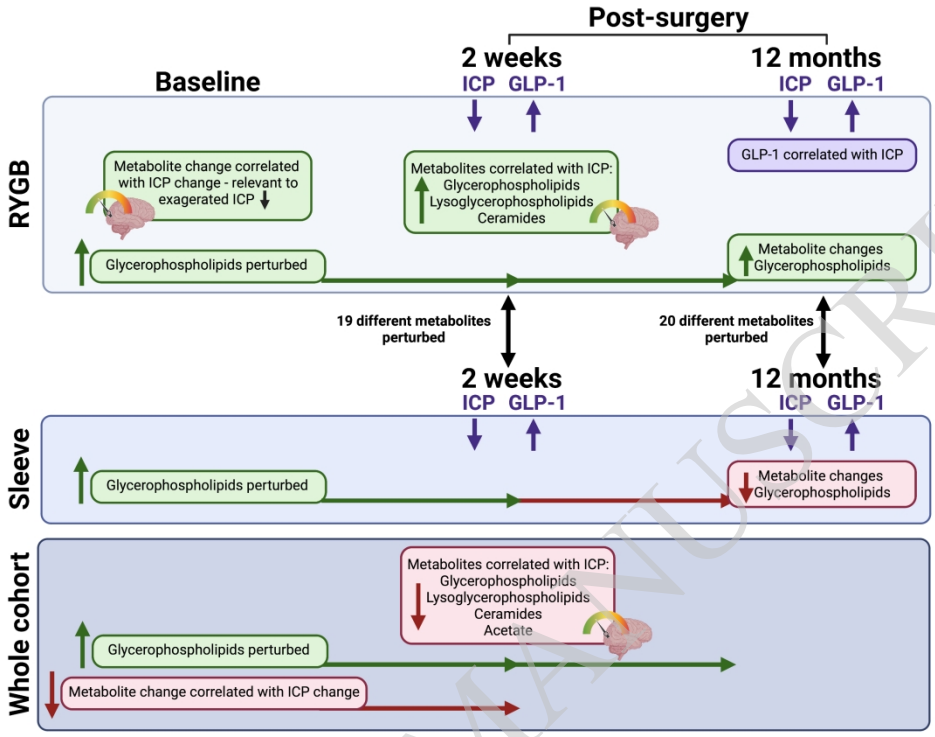

Figure 7

613x484mm (118 x 118 DPI)